Acta Mech 208, 117–131 (2009)
DOI 10.1007/s00707-008-0132-5

K. D. Kumar

Satellite attitude stabilization using fluid rings

Received: 20 August 2008 / Revised: 27 October 2008 / Published online: 8 January 2009

Abstract The three-dimensional attitude stabilization of a satellite using fluid rings is proposed in the present paper. The general formulation of the system that comprises a satellite and three fluid rings, one on each axis, is obtained through Euler's moment equations. The linearized system model is derived and the stability conditions are obtained. Linear control laws and nonlinear control laws based on sliding mode control techniques are developed for fluid control torques. The numerical simulation of the governing nonlinear equations of motion of the system along with stability analysis establishes the feasibility of achieving desired attitude stabilization of the satellite. The fluid controllers are successful in stabilizing the attitude of the satellite in presence of high attitude disturbance torques and intermittent actuators' failures. In the case of sudden attitude disturbance torques, the nonlinear fluid controllers outperform the linear fluid controllers with virtually no effect on the satellite attitude response. The proposed attitude stabilization method may find applications in future satellite missions.

List of symbols

A	cross-sectional area of the fluid ring, $\pi D^2/4$ (m^2)
C_1	$\rho\pi r^5/I_x$, a nondimensional fluid parameter
C_2	$\mu/(\rho r D\Omega)$, a nondimensional fluid parameter
C_3, C_4	$C_1\hat{D}^2/4, 8C_1C_2\hat{D}$
D	cross-sectional diameter of the fluid ring (m)
$\hat{D}$	D/r, dimensionless diameter of the fluid ring
f	Darcy–Wiesbach resistance coefficient
G	universal gravitational constant (m^3 kg^{-1} s^{-2})
I_k	principal centroidal moment of inertia of satellite about k-axis, $k = x, y, z$ (kg-m^2)
I_{kj}^f	principal centroidal moment of inertia of fluid ring-j about k-axis, $k = x, y, z$ (kg-m^2)
K_1, K_2	$(I_x - I_y)/I_z, (I_x - I_z)/I_y$; satellite mass distribution parameter
K_3, K_4	$I_y/I_x = (1 - K_1)/(1 - K_1K_2), I_z/I_x = (1 - K_2)/(1 - K_1K_2)$
K_{tj}^f	$\frac{I_{tj}^f}{I_x}, (t = x,\ y,\ z)$
K_t^f	$\sum_{j=1}^3 K_{tj}^f, (t = x,\ y,\ z)$
K_3^s, K_4^s	$K_3 + K_y^f, K_4 + K_z^f$

K. D. Kumar (✉)
Department of Aerospace Engineering, Ryerson University, 350 Victoria Street, Toronto, ON M5B-2K3, Canada
E-mail: kdkumar@ryerson.ca; krishnadevkumar@yahoo.com

M_E	Earth's mass (kg)
$\mathbf{U}_\beta$	external torque vector acting on the fluid motion (N m)
$\mathbf{u}_\beta$	$\mathbf{U}_\beta/(I_x\Omega^2)$
r	mean radius of the fluid ring (m)
R	orbital radius (m)
R_E	Earth radius (m)
R_n	Reynolds number, $\rho \mathrm{Dr}\dot{\beta}/\mu$ for circular fluid ring
S	system mass center
$S-\mathrm{X_0Y_0Z_0}$	coordinate axes in the local vertical frame
$S-\mathrm{XYZ}$	satellite body coordinate frame
U_j	fluid frictional torque about the jth fluid ring axis of symmetry (N m)
U_{cj}	fluid control torque applied by pump in the jth fluid ring (N m)
u_j, u_{cj}	$U_j/(I_x\Omega^2), U_{cj}/(I_x\Omega^2)$
α, ϕ, γ	satellite pitch, roll and yaw angles, respectively (deg)
$\alpha_d, \phi_d, \gamma_d$	desired or commanded satellite pitch, roll and yaw angles (deg)
$\alpha_0, \phi_0, \gamma_0$	α, ϕ, γ at $\theta = 0$ (deg)
$\alpha_0', \phi_0', \gamma_0'$	α', ϕ', γ' at $\theta = 0$
β_j, η_j	angular position and span of the fluid slug in the jth fluid ring, respectively (Fig. 2) (deg)
β_{je}	β_j at equilibrium (deg)
β_j'	angular speed of the fluid slug with respect to the fluid ring j (rad/s)
β_{j0}'	β_j' at $\theta = 0$
β_{j0}	β_j at $\theta = 0$ (deg)
β_0'	β_j' when $\beta_1' = \beta_2' = \beta_3'$ at $\theta = 0$
η_t	η_j when $\eta_1 = \eta_2 = \eta_3$ (deg)
ρ	fluid density (kg-m^{-3})
τ_j	shear stress for the fluid ring j (N m^{-2})
μ	viscosity of the fluid (kg m$^{-1}s^{-1}$)
θ	angle from the reference line (deg)
ω_i	angular rate of the satellite about the body fixed i-axis (rad/s)
Ω	orbit rate; $(\mathrm{GM_E/R^3})^{1/2}$ (rad/s)
$(.)_j$	(.) for the jth fluid ring, $j = 1,\ 2,\ 3$
$(.)_0, (.)_e$	(.) at $\theta = 0$, (.) at equilibrium
$(.)', (.)''$	$d(.)/d\theta$ and $d^2(.)/d\theta^2$, respectively
$(.)^\times$	skew-symmetric 3×3 matrix associated with (.) of 3×1 column matrix
$\lvert(.)\rvert_{\max}$	absolute maximum amplitudes of (.)

1 Introduction

The attitude stability of satellites is of considerable importance for successful completion of a space mission. Several methods of attitude stabilization [1–6] have been developed over the last four decades. The present paper considers fluid rings for three-dimensional attitude stabilization of a non-spinning satellite. In the past, viscous ring dampers [2,4,5] were applied for nutation damping of spin-stabilized satellites. The application of fluid loops has been discussed in some patents and papers [7–17]. An idea of using fluid moving in an enclosed circuit as a momentum storage device or gyroscope is mentioned in Ref. 7. Herman [8] described rotation of electrically conductive liquids in a closed circuit path by electromagnetic means for its application as a gyroscope. Wyatt and Swet [9] explained satellite yaw stabilization and propulsion using rotating toroidal tanks filled with fluid in liquid and vapor phases. The application of a rotator apparatus for spacecraft attitude control was considered by Rasmusson [10]. Marynard [11] presented a fluid momentum controller for neutralization and damping of external or internal periodic, non-accumulating torques acting on a spacecraft. An improved fluid actuating system for the control of spacecraft attitude was considered by Lurie et al. [12,13] The fluid loops might be located on the interior or exterior of the spacecraft. Iskenderian [14] presented a fluid-loop reaction ring that can control the attitude of a spacecraft by reacting against liquid contained in the loop.

One or several pumps, provided impetus to both the spacecraft and fluid, whereas hydraulic accumulators and valves were added to control flow. A method based on fluid loops was described by Laughlin et al. [15] for an attitude control of a spacecraft about a single axis. The fluid was driven by magnetohydro pumps. Gilbertson and Busch [16] presented a survey of micro-actuator technologies including electrohydrodynamics applicable to spacecraft. Recently, Kelly et al. [17] confirmed the feasibility of a fluidic momentum controller for spacecraft attitude control by conducting experiments aboard the NASA's KC-135A. Researchers at the department of aerospace engineering and engineering mechanics, University of Texas, Austin have been involved in testing of the fluidic momentum controller since 1987 [17]. Thus, the fluid loops/rings based attitude control systems can be utilized to stabilize librational dynamics of a satellite with a desired degree of accuracy and in comparison to the conventional reaction/momentum wheels or control moment gyros (CMGs), they have several advantages including large damping torque, light weight, and low cost. In addition, without adding significant weight to the system, the fluid loop radius can be varied according to the requirements of the satellite and mission; a large fluid loop with low fluid velocity and mass results in a highly energy efficient system with minimal vibration to the satellite structure. However, along with these advantages, there are several challenges associated with this system including modeling of fluid, fluid leakage, and thermal protection.

In the present investigation, we consider a satellite under gravity gradient torque along with the torque provided by fluid motion. The fluid motion without pump is just a passive damper to the gravity gradient satellite and therefore, it is pertinent here to review literature on the gravity gradient satellites with passive librational dampers. Several types of passive dampers have been applied to damp the libration of gravity gradient satellites [5,18–20]. Some of these are point-mass damper, damper mounted on external spring's boom, magnetic hysteresis rod damper, spherical tip damper, damping by boom articulation, and wheel damper. These dampers are in principle based on viscous fluids, mass-spring systems, eddy currents, or magnetic hysteresis or a combination of these. The details about these dampers are given in [5,18–20]. Without dampers, the attitude of a rigid satellite under gravity-gradient torque in a circular orbit remains infinitesimally stable in the Lagrange and Debra-Delp regions. However, in the presence of energy dissipation, the Debra-Delp region disappears and the attitude of the satellite remains infinitesimally as well as asymptotically stable in the Lagrange region only. The case of a point-mass linear damper positioned along the pitch axis of a satellite is illustrated in [5]. Recently, viscous ring dampers with commercial hydraulic oils (e.g., Tellus C5) have been considered for passive three-axis attitude control for a low-Earth orbit satellite in conjunction with a boom facilitating gravity-gradient torque for pitch and roll control, and a sail using aerodynamic torque for yaw control [21]. However, the suggested method takes a rather long time (on the order of 100s of orbital periods) to damp the attitude of the satellite.

In the past papers and patents [7–17,21] concerning fluid loop dampers, only conceptual descriptions and simple analyses based on angular momentum conservation are presented. The effect of gravity gradient torque on fluid loop controlled satellites, stability analysis, as well as the effectiveness of fluid loops/rings in controlling the satellite attitude in presence of attitude disturbances and actuators' failures have not been examined. In addition, the design of control laws including linear and nonlinear controllers has not been presented. These aspects are discussed in the present paper along with the detailed analyses of the system including stability analyses and numerical simulations. The system parameters are presented in dimensionless form so that the scope of application of the results no longer depends upon the particular satellite size, mass and inertia properties or fluid properties.

The system under study comprises of three fluid rings attached to a satellite at its three principal pitch, roll, and yaw axes, respectively (Fig. 1). The fluid inside the ring provides inherent damping to the satellite attitude motion. But as the damping torque is found to be low, it may take longer for the attitude motion of the satellite to reach desired attitude angles. With a view to stabilize the satellite attitude motion effectively, each fluid ring is equipped with a pump. A simple controller inside the pump is designed to regulate the fluid flow in each ring. The liquid propellant present in the satellite can be used in the fluid rings if feasible; otherwise a different fluid could be supplied.

The body of this paper consists of six main sections followed by a conclusion. Section 2 presents a general formulation of the system. The Euler's moment equations are used to obtain the governing ordinary differential equations of motion for the proposed system. In Sect. 3, the linearized system model is derived and the stability analysis is presented. The control laws are derived in Sect. 4. Finally, for a detailed assessment of the proposed attitude stabilization strategy, the set of governing equations of motion is numerically integrated and the effects of various system parameters on the system response are examined in Sect. 5.

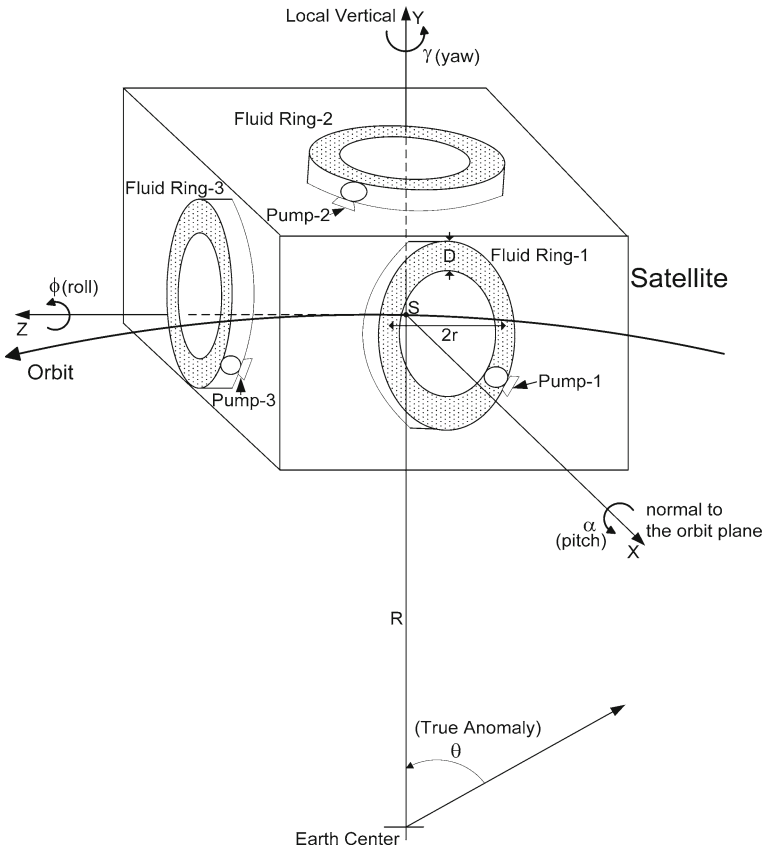

Fig. 1 Orbiting satellite with fluid rings

2 Proposed system model and equations of motion

The system model comprises a satellite and three fluid rings (Fig. 1). Each fluid ring is fitted with a pump to regulate the flow of the fluid. The system center of mass 'S' lies on the center of mass of the satellite. As the focus is on studying the effects of fluid motion on the satellite attitude, the distance of the fluid ring from the center of mass is assumed negligible. The coordinate frame $X_oY_oZ_o$ passing through the system center of mass S represents the orbital reference frame. Here the X_o-axis is taken along the normal to the orbital plane, the Y_o-axis points along the local vertical and the Z_o-axis represents the third axis of this right handed frame taken. The orientation of the satellite is specified by a set of three successive rotations: α (pitch) about the X_0-axis, ϕ about the new roll axis (Z-axis, if $\alpha = 0$), and finally γ about the resulting yaw axis. The corresponding principal body-fixed coordinate frame for the satellite is denoted by S-XYZ. For the fluid ring j, the angle β_j denotes rotation of the fluid slug about the j-axis ($j = 1, 2, 3$ corresponds to the X-axis, Y-axis, and Z-axis, respectively) with respect to the body-fixed Y-axis (Fig. 2). The resulting coordinate frame associated with this vector is denoted by $S_{Lj} - X_{Lj}Y_{Lj}Z_{Lj}$. The system under consideration has six generalized coordinates: three for the satellite rotations: pitch(α), roll(ϕ) and yaw(γ), and three for the fluid rings: β_j, $j = 1, 2, 3$. As the fluid ring is very small compared to the satellite, its product of inertia and center of mass movement effects are ignored. We assume fully filled fluid rings (i.e., $\eta_j = 2\pi$) as shown in Fig. 2. The moments of inertia of the fluid ring are obtained as

$$\begin{aligned} &I^f_{x1} = 2\pi\rho Ar^3, \quad I^f_{y1} = I^f_{z1} = \pi\rho Ar^3, \quad I^f_{x2} = \pi\rho Ar^3, \quad I^f_{y2} = 2\pi\rho Ar^3, \\ &I^f_{z2} = \pi\rho Ar^3, \quad I^f_{x3} = I^f_{y3} = \pi\rho Ar^3, \quad I^f_{z3} = 2\pi\rho Ar^3. \end{aligned} \tag{1}$$

The motion of the fluid relative to the annular ring causes energy dissipation through shear stress acting on the wall of the ring. The shear stress τ_j for the fluid ring j is given as

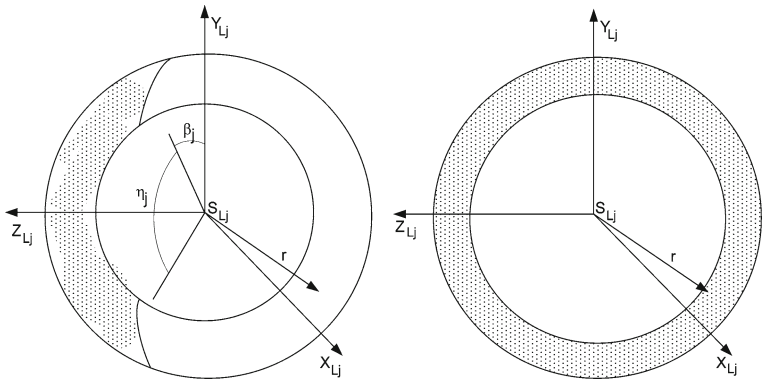

Fig. 2 **a** This part illustrates the angular position β_j and span η_j of the fluid slug in the jth fluid ring. **b** This part illustrates a filled fluid ring with $\eta_j = 2\pi$

$$\tau_j = \frac{1}{8} f \rho V^2 = \frac{1}{8} f \rho r^2 \dot{\beta}_j^2, \tag{2}$$

where laminar flow inside the fluid ring is assumed ($R_n < 2000$) [22],

$$f = \frac{64}{R_n}. \tag{3}$$

We neglect end effects as they do not have much significance in the present analysis; further, to simplify integration of shear stress over the wetted area of the ring, we assume $D \ll r$. The resulting fluid torque U_{fj} about the ring axis of symmetry is

$$U_{fj} = -\text{sign}(\dot{\beta}_j)\pi \tau_j r^2 D \eta_j, \quad j = 1, 2, 3. \tag{4}$$

Applying Euler's momentum equations, the governing nonlinear coupled ordinary differential equations of motion of the system are obtained as

$$I_s \dot{\omega}_s + \omega_s^{\times} I_s \omega_s + \dot{h}_f + \omega_s^{\times} h_f, = 3 \left(\frac{\mu}{\mathbf{R}^3} \right) \mathbf{C_s}^{\times} (\mathbf{I_s} + \mathbf{I_f}) \mathbf{C_s}, \tag{5}$$

$$\dot{h}_f + \omega_s^{\times} h_f = \mathbf{U}_{\beta}, \tag{6}$$

where

$$\mathbf{I_s} = \begin{pmatrix} I_x & 0 & 0 \\ 0 & I_y & 0 \\ 0 & 0 & I_z \end{pmatrix}, \quad \mathbf{h_f} = \begin{bmatrix} h_x \\ h_y \\ h_z \end{bmatrix} = \begin{bmatrix} \sum_{j=1}^{3} I_{xj}^f \omega_x + I_{x1}^f \dot{\beta}_1 \\ \sum_{j=1}^{3} I_{yj}^f \omega_y + I_{y2}^f \dot{\beta}_2 \\ \sum_{j=1}^{3} I_{zj}^f \omega_z + I_{z3}^f \dot{\beta}_3 \end{bmatrix}, \quad \mathbf{I_f} = \begin{pmatrix} \sum_{j=1}^{3} I_{xj} & 0 & 0 \\ 0 & \sum_{j=1}^{3} I_{yj} & 0 \\ 0 & 0 & \sum_{j=1}^{3} I_{zj} \end{pmatrix}, \tag{7}$$

$$\boldsymbol{\omega}_s = \begin{bmatrix} \omega_x \\ \omega_y \\ \omega_z \end{bmatrix} = \begin{bmatrix} (\dot{\theta} + \dot{\alpha}) \cos\phi \cos\gamma - \dot{\phi} \sin\gamma \\ -(\dot{\theta} + \dot{\alpha}) \sin\phi + \dot{\gamma} \\ (\dot{\theta} + \dot{\alpha}) \cos\phi \sin\gamma + \dot{\phi} \cos\gamma \end{bmatrix}, \quad \boldsymbol{\omega}_s{}^{\times} = \begin{pmatrix} 0 & -\omega_z & \omega_y \\ \omega_z & 0 & -\omega_x \\ -\omega_y & \omega_x & 0 \end{pmatrix}, \tag{8}$$

$$\mathbf{C_s} = \begin{bmatrix} C_x \\ C_y \\ C_z \end{bmatrix} = \begin{bmatrix} \cos\alpha \sin\phi \cos\gamma + \sin\alpha \sin\gamma \\ \cos\alpha \cos\phi \\ \cos\alpha \sin\phi \sin\gamma - \sin\alpha \cos\gamma \end{bmatrix}. \tag{9}$$

The $\mathbf{U}_\beta$ in Eq. (6) is an external torque vector acting on the fluid motion given as

$$\mathbf{U}_\beta = \begin{bmatrix} U_{f1} + U_{c1} \\ U_{f2} + U_{c2} \\ U_{f3} + U_{c3} \end{bmatrix}, \tag{10}$$

where U_{fj}, $j = 1, 2, 3$, denotes fluid frictional torque and U_{cj}, $j = 1, 2, 3$, is the fluid control torque applied by the pump.

It is convenient to replace t by θ as the independent variable and to denote derivatives with respect to θ by primes using the following relations:

$$\dot{\mathbf{q}} = \dot{\theta}\,\mathbf{q}' = \sqrt{\frac{GM_E}{R^3}}\mathbf{q}', \quad \ddot{\mathbf{q}} = \frac{GM_E}{R^3}\mathbf{q}'', \tag{11}$$

where $\mathbf{q}$ is an independent system coordinate vector given as $\mathbf{q} = \left[\alpha\ \gamma\ \phi\ \beta_1\ \beta_2\ \beta_3\right]^T$.

For convenience of system representation and response simulation, we consider the following dimensionless system parameters:

$$\hat{D} = \frac{D}{r}, \quad C_1 = \frac{\rho\pi r^5}{I_x}, \quad C_2 = \frac{\mu}{\rho r D\Omega}, \tag{12}$$

besides K_1 and K_2 describing satellite mass moment of inertia properties. The other parameters in the equations of motion are expressed in terms of these parameters as

$$u_{fj} = -\text{sign}(\beta_j')\frac{fC_1\hat{D}}{8}\beta_j'^2\eta_j, \tag{13}$$

$$\frac{\rho\pi r^3}{I_x} = \frac{C_1\hat{D}^2}{4}, \tag{14}$$

$$R_n = \frac{\rho D r\dot{\beta}_j}{\mu} = \frac{\beta_j'}{C_2}. \tag{15}$$

$\mathbf{U}_\beta$ in Eq. (6) is replaced by

$$\mathbf{u}_\beta = \begin{bmatrix} u_{\beta_1} \\ u_{\beta_2} \\ u_{\beta_3} \end{bmatrix} = \left(\frac{U_\beta}{I_x\Omega^2}\right) = \begin{bmatrix} u_{f1} + \mathrm{u}_{c1} \\ u_{f2} + \mathrm{u}_{c2} \\ u_{f3} + \mathrm{u}_{c3} \end{bmatrix}. \tag{16}$$

The governing equations of motion after carrying out considerable algebraic manipulation and nondimensionalization are written in matrix notation as

$$M(\mathbf{q}, \theta, K_1, K_2)\mathbf{q}'' + F(\mathbf{q}, \mathbf{q}', \theta, K_1, K_2) = \mathbf{u}_q, \tag{17}$$

where $M(\mathbf{q}, \theta, K_1, K_2)$ is the mass matrix and $F(\mathbf{q}, \mathbf{q}', \theta, K_1, K_2)$ is the vector containing all the linear and nonlinear terms including the Coriolis and centrifugal contributions.

3 Linear system model and stability analysis

With a view to understand the system dynamics, we first obtain the equilibrium state of the system, and then linearize the equations of motion of the system about this equilibrium state. By substitution of the equilibrium conditions defined by

$$\mathbf{q}'' = \mathbf{q}' = 0 \tag{18}$$

into Eqs. (17) and assuming a fully filled fluid situation (i.e., $\eta_1 = \eta_2 = \eta_3 = \eta_t = 2\pi$), we find the equilibrium state of the system as

$$\alpha_e = \phi_e = \gamma_e = \alpha_e' = \phi_e' = \gamma_e' = 0, \quad \beta_{je}' = 0, \quad j = 1, 2, 3. \tag{19}$$

Next we linearize Eqs. (17) about the equilibrium state given by Eq. (19). The resulting equations of motion of the system are obtained as follows:

$$\mathbf{M_p q_p''} + \mathbf{K_p q_p} = \mathbf{u}_p, \tag{20}$$

$$\mathbf{M}_r \mathbf{q}_r'' + \mathbf{G_r q}_r' + \mathbf{K_r q}_r = \mathbf{u}_r, \tag{21}$$

where

$$\mathbf{q_p} = [\alpha\ \beta_1]^T, \quad \mathbf{M_p} = \begin{bmatrix} 1 & 0 \\ 0 & 1 \end{bmatrix}, \quad \mathbf{K_p} = \begin{bmatrix} -3(K_3 - K_4) & 0 \\ 6(K_3 - K_4) & 0 \end{bmatrix}, \quad \mathbf{u_p} = \begin{bmatrix} -u_{\beta 1} \\ \left(2 + \frac{1}{C_3 \eta_t}\right) u_{\beta 1} \end{bmatrix},$$

$$\mathbf{q_r} = \begin{bmatrix} \gamma & \phi & \beta_2 & \beta_3 \end{bmatrix}^T, \quad \mathbf{M_r} = \begin{bmatrix} K_3 & 0 & 0 & 0 \\ 0 & K_4 & 0 & 0 \\ 0 & 0 & K_3 & 0 \\ 0 & 0 & 0 & K_4 \end{bmatrix}, \quad \mathbf{G_r} = \begin{bmatrix} 0 & 1 - K_3 - K_4 & 0 & 0 \\ -1 + K_3 + K_4 & 0 & 0 & 0 \\ 0 & 2(-1 + K_4) & 0 & -K_3 \\ 2(1 - K_3) & 0 & K_4 & 0 \end{bmatrix},$$

$$\mathbf{K_r} = \begin{bmatrix} 1 - K_4 & 0 & 0 & 0 \\ 0 & 4(1 - K_3) & 0 & 0 \\ -2(1 - K_4) & 0 & 0 & 0 \\ 0 & -8(1 - K_3) & 0 & 0 \end{bmatrix}, \quad \mathbf{u_r} = \begin{bmatrix} -u_{\beta 2} \\ -u_{\beta 3} \\ \left(2 + \frac{K_3}{C_3 \eta_t}\right) u_{\beta 2} \\ \left(2 + \frac{K_4}{C_3 \eta_t}\right) u_{\beta 3} \end{bmatrix};$$

$$\mathbf{u}_\beta = \mathbf{u}_f + \mathbf{u}_c, \quad \mathbf{u}_f = \begin{bmatrix} u_{f1} & u_{f2} & u_{f3} \end{bmatrix}^T, \quad \mathbf{u}_c = [u_{c1} \quad u_{c2} \quad u_{c3}]^T.$$

Using Eqs. (3), (13) and (15), we rewrite $\mathbf{u}_f$ as

$$u_{fj} = -C_4 \beta_j', \quad j = 1, 2, 3, \tag{22}$$

where $C_4 = 8 C_1 C_2 \hat{D} \eta_t$.

As per the preceding linear equations of motion (Eqs. (20) and (21)), the pitch motion of the system is decoupled from the system roll and yaw motion. So, we first analyze the stability of the pitch motion of the system. The characteristic equation of the system pitch motion is obtained as

$$s^3 + \left[\left(2 + \frac{1}{C_3 \eta_t}\right) C_4 \eta_t\right] s^2 + \left[\frac{3(K_1 - K_2)}{1 - K_1 K_2}\right] s + \frac{3(K_1 - K_2) C_4}{C_3 (1 - K_1 K_2)} = 0, \tag{23}$$

where $\eta_t = 2\pi$.

Applying the Routh–Hurwitz criterion, the conditions for system pitch stability can be stated as follows:

$$K_1 > K_2. \tag{24}$$

For the system roll and yaw motion, the characteristic equation can be obtained as

$$s^6 + p_1 s^5 + p_2 s^4 + p_3 s^3 + p_4 s^2 + p_5 s + p_6 = 0, \tag{25}$$

where

$$p_1 = \frac{2}{K_3 K_4 C_3} [(K_3 + K_4) C_3 + K_3 K_4] C_4,$$

$$p_2 = \frac{1}{K_3 K_4 C_3} \left\{(1 + 2K_3 - K_4 + 3K_3 K_4 - 3K_3^2) C_3 + C_4 [4 C_3 C_4 + 2(K_3 + K_4) C_4] + C_4^2 K_4 K_3\right\}$$

$$p_3 = \frac{1}{K_3K_4C_3}[4K_3K_4 + 2 + 10C_3 + 4K_3 - 6K_3C_3 - 6K_3^2 - 2K_4]C_4,$$

$$p_4 = \frac{1}{K_3K_4C_3^2}\{[4C_4^2 - 3K_3^2 + 6K_3K_4 + 5 - 5K_4 - 2K_3]C_3^2$$

$$+(2K_4K_3 - K_4 + 1 + 2C_3K_4 - 4C_3K_3 + 6C_3 + 2K_3 - 3K_3^2)C_4^2\},$$

$$p_5 = \frac{1}{K_3K_4C_3}[8K_4K_3 + 8 - 8K_3 - 8K_4 + (10 - 8K_3 - 2K_4)C_3]C_4,$$

$$p_6 = -\frac{4}{K_3K_4C_3^2}[-1 + K_3 + K_4 - K_3K_4](C_3^2 + C_4^2).$$

Applying the Routh-Hurwitz criterion, the conditions for the system roll and yaw stability can be obtained as

$$\begin{aligned}
&p_j > 0, \quad j = 1, 2, ..., 6,\\
&p_2 - \frac{p_3}{p_1} > 0,\\
&p_2 - \frac{p_3}{p_1} > \frac{p_1}{p_3}\left[p_4 - \frac{p_5}{p_1}\right],\\
&\left[p_3\left(p_2 - \frac{p_3}{p_1}\right)\left(p_4 - \frac{p_5}{p_1}\right) - p_1\left(p_4 - \frac{p_5}{p_1}\right)^2\right] > \left[p_5\left(p_2 - \frac{p_3}{p_1}\right) - p_1p_6\right],\\
&\left[p_5\left(p_2 - \frac{p_3}{p_1}\right) - p_1p_6\right]\left\{\left(p_2 - \frac{p_3}{p_1}\right)\left[p_1p_6 + p_3\left(p_4 - \frac{p_5}{p_1}\right)\right] - p_1\left(p_4 - \frac{p_5}{p_1}\right)^2\right.\\
&\left. - p_5\left(p_2 - \frac{p_3}{p_1}\right)^2\right\} > p_6\left(p_2 - \frac{p_3}{p_1}\right)\left[p_3\left(p_2 - \frac{p_3}{p_1}\right) - p_1\left(p_4 - \frac{p_5}{p_1}\right)\right].
\end{aligned} \tag{26}$$

The condition of stability reduces to

$$K_1K_2 > 0. \tag{27}$$

The conditions (24) and (27) clearly state that the proposed system with natural damping is only stable in the region specified by $K_1 > K_2$, $K_1 > 0$, $K_2 > 0$, also called *Lagrange region*. In fact, this result coincides with the result we know about the stability of gravity-gradient satellite in the presence of energy dissipation [5].

4 Control laws

In order to apply a suitable variation of fluid torque $\mathbf{u_c}$ to achieve desired satellite attitude response, we develop linear and nonlinear control laws. These laws are derived based on the linear system (Eqs. (20) and (21)). Linear control laws are designed first followed by the development of nonlinear control laws based on sliding mode control techniques [23].

4.1 Linear control laws

We assume the Lyapunov function for the system as

$$V(x) = \frac{1}{2}\mathbf{S}^T\mathbf{S}, \tag{28}$$

where

$$\mathbf{S} = [S_1 \quad S_2 \quad S_3]^T = \mathbf{q}_s' + \boldsymbol{\lambda}\mathbf{q}_s \tag{29}$$

with $\lambda = \text{diag}\,(\lambda_1, \quad \lambda_2, \quad \lambda_3) > 0$, $\mathbf{q_s} = \begin{bmatrix}\alpha & \gamma & \phi\end{bmatrix}^T$.

Differentiating Eq. (28) with respect to θ and using Eq. (29) yields

$$V'(x) = \mathbf{S^T S'} = \mathbf{S^T}\left(\mathbf{q}_s'' + \boldsymbol{\lambda}\mathbf{q}_s'\right). \tag{30}$$

Taking

$$\mathbf{S'} = \mathbf{q}_s'' + \boldsymbol{\lambda}\mathbf{q}_s' = -\boldsymbol{\kappa} S \tag{31}$$

into Eq. (30) proves

$$V' = -\boldsymbol{\kappa}\mathbf{S}^2 \leq 0, \tag{32}$$

where $\boldsymbol{\kappa} = \text{diag}\,(\kappa_1, \kappa_2, \kappa_3)$.

Equation (31) can be rewritten as

$$\mathbf{q}_\mathbf{s}'' + (\boldsymbol{\lambda} + \boldsymbol{\kappa})\mathbf{q_s} + \boldsymbol{\kappa}\boldsymbol{\lambda}\mathbf{q_s} = 0. \tag{33}$$

Comparing the preceding Eq. (33) with the desired performance specified by the second order linear system with the given closed-loop damping ratios, $\boldsymbol{\xi}_\mathbf{c} = \text{diag}\,(\xi_{c1}, \xi_{c2}, \xi_{c3})$ and frequencies, $\boldsymbol{\omega}_\mathbf{c} = \text{diag}\,(\omega_{c1}, \omega_{c2}, \omega_{c3})$:

$$\mathbf{q}_\mathbf{s}'' + 2\boldsymbol{\xi}_\mathbf{c}\boldsymbol{\omega}_\mathbf{c}\mathbf{q}_\mathbf{s}' + \boldsymbol{\omega}_\mathbf{c}^\mathbf{2}\mathbf{q_s} = 0 \tag{34}$$

and assuming critical damping $\xi_{cj} = 1$, j = 1,2,3, yields

$$\lambda_j = \kappa_j = \omega_{jc}, \quad j = 1, 2, 3. \tag{35}$$

Referring to Eq. (31) and substituting for $\mathbf{q}_s''$ using Eqs. (20) and (21), the control laws are obtained as

$$\mathbf{u}_c = (2\mathbf{K}_t\boldsymbol{\omega}_\mathbf{c} + \mathbf{G_s})\mathbf{q'}_\mathbf{s} + (\mathbf{K}_t\boldsymbol{\omega}_\mathbf{c}^\mathbf{2} + \mathbf{K_s})\mathbf{q_s} - \mathbf{u}_f, \tag{36}$$

where

$$\boldsymbol{G}_s = \begin{bmatrix} 0 & 0 & 0 \\ 0 & 0 & -1 + K_3 + K_4 \\ 0 & 1 - K_3 - K_4 & 0 \end{bmatrix}, \quad \mathbf{K}_s = \begin{bmatrix} 3(K_3 - K_4) & 0 & 0 \\ 0 & -(1 - K_4) & 0 \\ 0 & 0 & -4(1 - K_3) \end{bmatrix},$$

$$\mathbf{K}_t = \begin{bmatrix} 1 & 0 & 0 \\ 0 & K_3 & 0 \\ 0 & 0 & K_4 \end{bmatrix}.$$

Note that the desired attitude angles and their corresponding rates are assumed null.

4.2 Nonlinear control laws

Assuming the Lyapunov function given by Eq. (28) and differentiating it with respect to θ yields (see Eq. (30))

$$V'(x) = \mathbf{S^T S'} = \mathbf{S^T}\left(\mathbf{q}_s'' + \boldsymbol{\lambda}\mathbf{q}_s'\right). \tag{37}$$

Taking

$$\mathbf{S'} = \mathbf{q}_s'' + \boldsymbol{\lambda}\mathbf{q}_s' = -\boldsymbol{\eta}\text{sgn}(\mathbf{S}) \tag{38}$$

into Eq. (37) proves

$$V' = -\boldsymbol{\eta}|\mathbf{S}| \leq 0, \tag{39}$$

where $\boldsymbol{\eta} = \text{diag}\,(\eta_1, \eta_2, \eta_3)$.

Taking $\lambda_j = \lambda_{sj}$, $j = 1, 2, 3$, and referring to Eq. (38) and substituting for $\mathbf{q}_s''$ using Eqs. (20) and (21), the control laws are obtained as

$$\mathbf{u}_c = (\mathbf{K}_t\boldsymbol{\lambda}_s + \mathbf{G_s})\mathbf{q}_\mathbf{s}' + \mathbf{K_s}\mathbf{q_s} + \mathbf{K}_t\boldsymbol{\eta}\text{sgn}(\mathbf{S}) - \mathbf{u}_f. \tag{40}$$

Table 1 System parameters and initial conditions for numerical simulation

Satellite orbit	6,878 km
Satellite mass moments of inertia	$I_x = 0.027$, $I_y = 0.022$, $I_z = 0.016$(kg-m^2)
Fluid ring	$r = 8.8$ cm, $D = 3.52$ cm, $\eta_1 = \eta_2 = \eta_3 = \eta_t = 2\pi$
Working fluid	Freon 11 ($\rho = 1,459\,\mathrm{kg\,m^{-3}}$; $\mu = 5 \times 10^{-4}\,\mathrm{kg\,m^{-1}s^{-1}}$ at 20°C)
Maximum fluid discharge rate	$5 \times 10^{-4}\,\mathrm{m^3 s^{-1}}$
Control parameters	$\xi_{cj} = 1, \omega_{cj} = 1.5, \lambda_j = \kappa_j = \omega_{cj}, \lambda_{sj} = 1, \eta_j = 0.4, \delta_j = 0.01, j = 1, 2, 3$
Initial conditions	$\alpha_0 = 20$ deg, $\phi_0 = -15$ deg, $\gamma_0 = 25$ deg, $\alpha'_0 = \phi'_0 = \gamma'_0 = 0.1$;
	$\beta_{j0} = 0, \beta'_{j0} = 10^{-30}, j = 1, 2, 3$

In order to avoid chattering [4], the signum function used in Eq. (40) is replaced by a saturation function as follows:

$$\mathrm{sgn}(S_j) \approx \mathrm{sat}\left(\frac{S_j}{\delta_j}\right) = \begin{cases} \mathrm{sgn}(S_j) & \text{for } |S_j| > \delta_j, \quad j = 1, 2, 3, \\ \frac{S_j}{\delta_j} & \text{for } |S_j| \le \delta_j, \quad j = 1, 2, 3, \end{cases} \tag{41}$$

where $\delta_j > 0$, $j = 1, 2, 3$, represents the boundary layer. Thus, the resulting nonlinear control laws can be expressed as

$$\mathbf{u_c} = (\mathbf{K}_t \boldsymbol{\lambda}_s + \mathbf{G_s})\mathbf{q}'_\mathbf{s} + \mathbf{K_s q_s} + \mathbf{K}_t \boldsymbol{\eta}\,\mathrm{sat}\left(\frac{\mathbf{S}}{\boldsymbol{\delta}}\right) - \mathbf{u} \tag{42}$$

or in terms of components

$$u_{1c} = \eta_1 \mathrm{sat}\left(\frac{S_1}{\delta_1}\right) + \lambda_{s1}\alpha' + 3(K_3 - K_4)\alpha - u_1, \tag{43}$$

$$u_{2c} = K_3\left[\lambda_{s2}\gamma' + \eta_2 \mathrm{sat}\left(\frac{S_2}{\delta_2}\right)\right] - (1 - K_3 - K_4)\phi' - (1 - K_4)\gamma - u_2, \tag{44}$$

$$u_{3c} = K_4\left[\lambda_{s3}\phi' + \eta_3 \mathrm{sat}\left(\frac{S_3}{\delta_3}\right)\right] - (-1 + K_3 + K_4)\gamma' - 4(1 - K_3)\phi - u_3. \tag{45}$$

5 Results and discussion

In order to study the performance of the proposed system, the detailed system response is simulated numerically using Eqs. (17) with the initial conditions given in Table 1. The dimensionless system parameters (12) referring to Table 1 are $K_1 = 0.5$, $K_2 = 0.3125$, $\hat{D} = 0.4$, $C_1 = 0.8959$ and $C_2 = 0.1$. In each of the fluid rings, 0.1076 liter of working fluid (Freon 11) with a mass of 0.157 kg is used (Table 1). The desired satellite attitude angles ($\alpha_d, \phi_d, \gamma_d$) and corresponding rates are null. The attitude control response settling time (1% of steady-state value) is assumed to be 0.5 orbit period; this corresponds to controller parameters (Eq. 35) using the relation $t_{js} = 4.6/(2\pi\xi_{jc}\omega_{jc}) = 0.5$ as $\xi_{jc} = 1, \omega_{jc} = 1.5, \lambda_j = \kappa_j = \omega_{jc}$, $j = 1, 2, 3$. The integration is carried out using the International Mathematical and Statistical Library (IMSL) routine DDASPG based on the Petzold-Gear BDF method [24].

We first consider the system moving in a circular orbit (i.e., e = 0) and study the dynamics of the system with natural damping (i.e., $u_j \neq 0, u_{cj} = 0$, $j = 1, 2, 3$). The attitude angles of the satellite are found to be asymptotically stable (Fig. 3). Note that the satellite without fluid rings has undamped attitude oscillations of pitch frequency $\omega = \sqrt{3(K_1 - K_2)/(1 - K_1 K_2)} = 0.8165$ rad/s and coupled roll and yaw frequencies $\omega_{1,2} = \sqrt{(1 + 3K_1 + K_1K_2)\left[1 \pm \sqrt{1 - 16K_1K_2/(1 + 3K_1 + K_1K_2)^2}\right]/2} = 0.5108$ rad/s (first harmonic), 1.5477 rad/s (second harmonic). In the case of the system with fluid rings, the maximum value of Reynold's number (referring to Eq. (15)) is found to be below 1 and thus, it justifies the assumption of laminar flow in

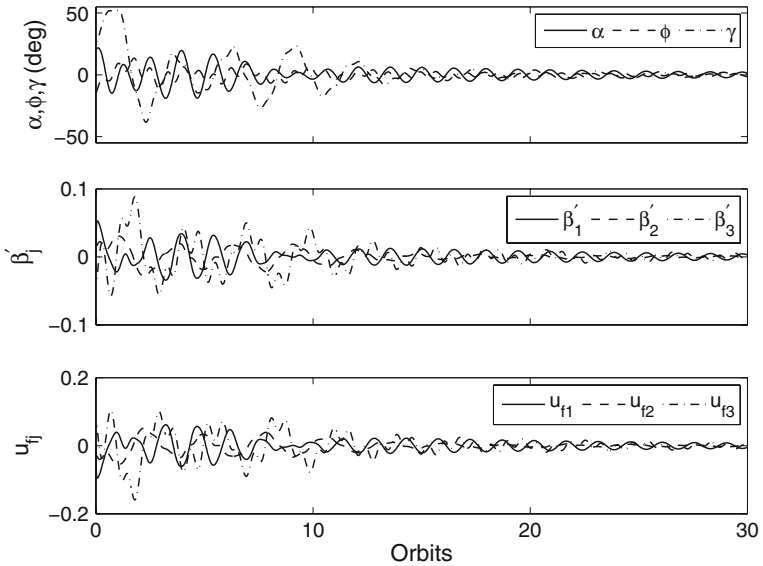

Fig. 3 Satellite attitude response without fluid controller torques ($\mathbf{u_c} = 0$)

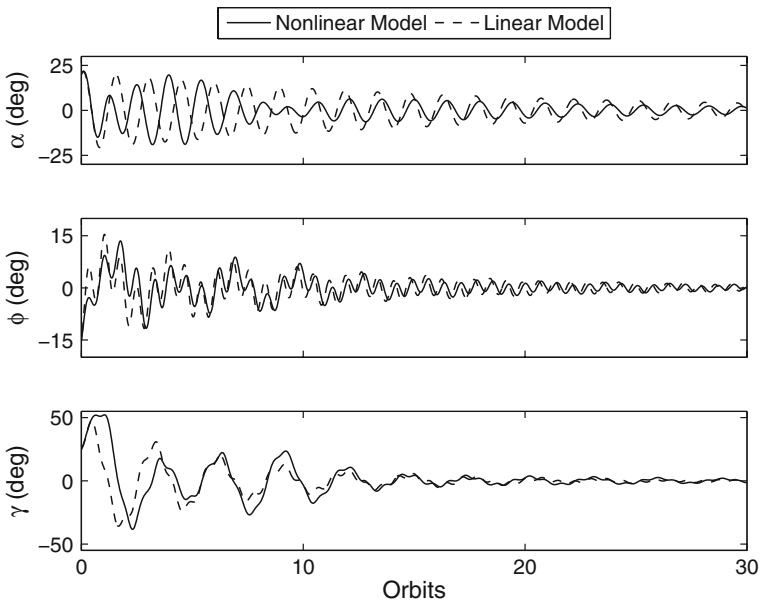

Fig. 4 Comparison between responses of linear and nonlinear system models without fluid controller torques ($\mathbf{u_c} = 0$)

the fully filled rings. The nonlinear system response is compared to the response of the linear system (20–21) as shown in Fig. 4. The linear response matches well with the nonlinear response and all the eigenvalues of the linear system have negative real parts (pitch motion: $-11.58, -0.01 \pm 0.68j$; roll and yaw motion: $-13.38, -13.04, -0.01 \pm 1.38j, -0.03 \pm 0.35j$), proving asymptotically stable system response. Further numerical simulations show that the system is stable only in the Lagrange region (i.e., $K_1 > K_2, K_1 > 0, K_2 > 0$), which confirms the stability conditions as per Eqs. (24) and (27).

In fact, the system with natural damping (see Figs. 3, 4) takes a rather long time in the order of tens of orbits to reach steady-state, and, therefore, we consider a fluid controller u_{cj} as per control laws given by Eqs. (23). Figure 5 shows the satellite attitude response with linear fluid controllers. The linear controllers (as per Eq. (36)) are successful in stabilizing the satellite attitude within half an orbit. The fluid flow remains laminar with $R_n < 22$ and the maximum fluid discharge rate is only $2.1 \times 10^{-7}\,\mathrm{m}^3/\mathrm{s}$. In the case when nonlinear

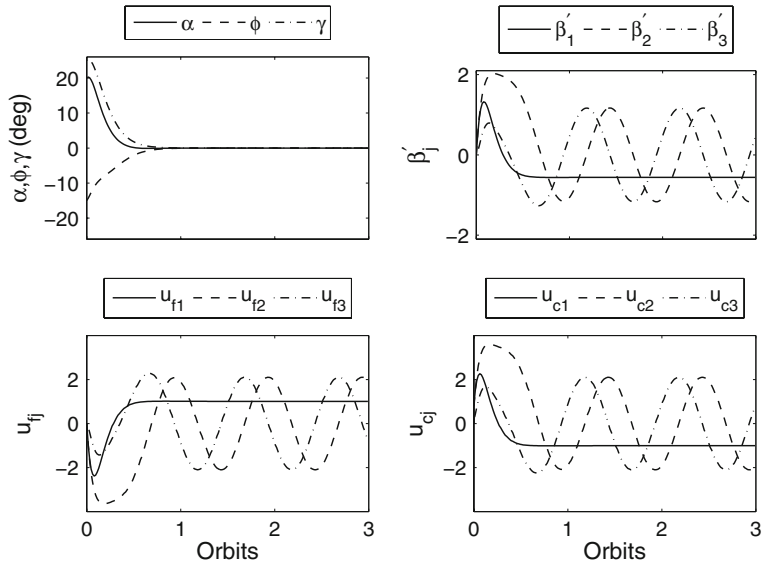

Fig. 5 Satellite attitude performance as affected by linear fluid controllers

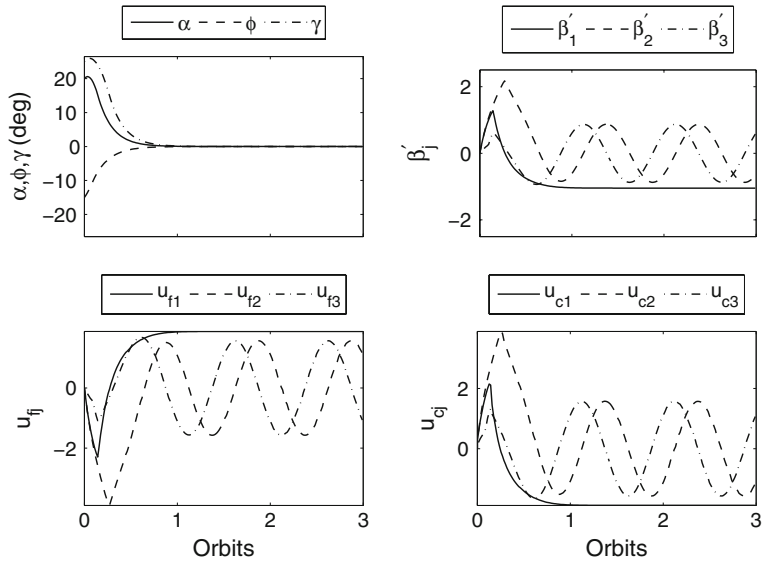

Fig. 6 Satellite attitude performance as affected by nonlinear fluid controllers

controllers (as per Eq. (37)) are applied, similar satellite attitude performance is obtained (Fig. 6) except that there are slight variations in fluid torques and flow rates. Thus, the linear and nonlinear fluid controllers are successful in achieving desired satellite attitude performance.

Next the effect of external disturbance torques on the controller performance response is examined (Fig. 7). Both linear and nonlinear controllers are successful in stabilizing the satellite attitude within half an orbit; in other words, the satellite attitude remains virtually unaffected by the presence of external disturbance torques. However, in the case of sudden external disturbances as might be encountered in real space missions (Fig. 8), the satellite attitude response using the nonlinear controllers remains virtually unaffected, while applying the linear controllers the satellite attitude response deteriorates during external disturbances, reaching the maximum attitude angles of $|\alpha|_{\max} = 2.45$ deg, $|\phi|_{\max} = 3.27$ deg, and $|\gamma|_{\max} = 4.36$ deg.

The effect of actuators' failures on the controller performance is studied next (Fig. 9). Even though pitch, roll and yaw controllers are switched off from 1 to 2 orbits, both the linear and nonlinear controllers are able to stabilize the satellite attitude within half an orbit after the controllers are switched on at the 2nd orbit. The

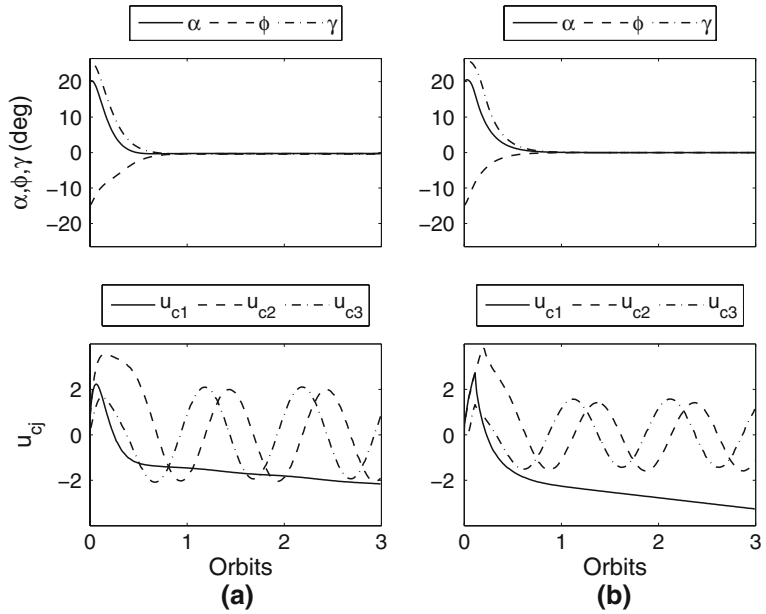

Fig. 7 Satellite attitude response as affected by external disturbance torques ($u_1 = u_2 = u_3 = 0.01$): **a** linear controllers and **b** nonlinear controllers

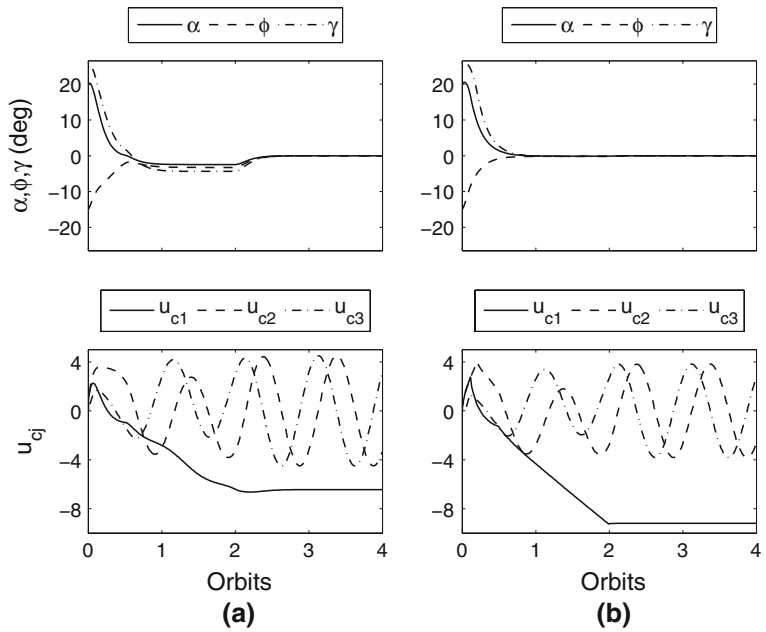

Fig. 8 Satellite attitude response as affected by sudden external disturbances from 0.5 to 2 orbits: **a** linear controllers and **b** nonlinear controllers

maximum attitude errors are $|\alpha|_{\max} = 6.421$ deg, $|\phi|_{\max} = 9.845$ deg, and $|\gamma|_{\max} = 23.91$ deg using the linear controllers, while the nonlinear controllers result in attitude errors of $|\alpha|_{\max} = 11.78$ deg, $|\phi|_{\max} = 7.761$ deg, and $|\gamma|_{\max} = 13.64$ deg.

6 Conclusions

The attitude stabilization of a satellite using fluid rings is presented in this paper. Results of the numerical integration of the governing nonlinear equations of motion along with their verification through stability anal-

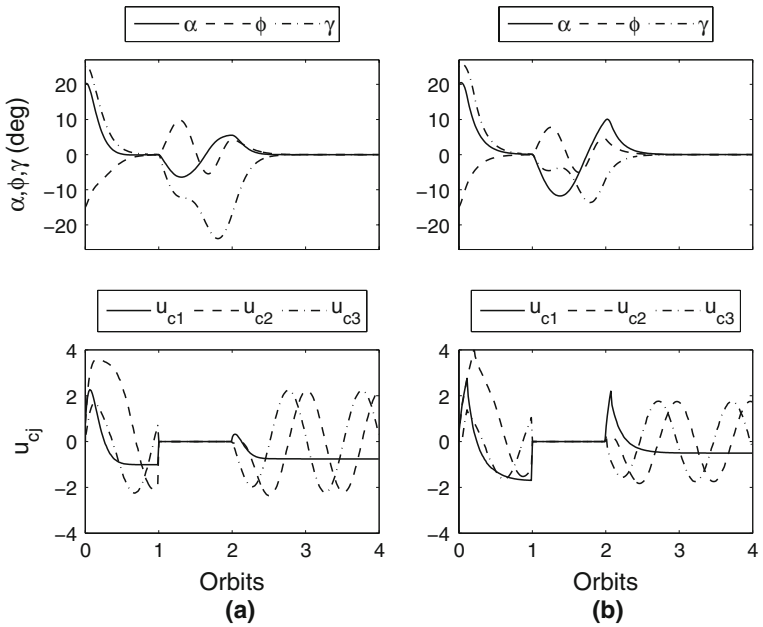

Fig. 9 Satellite attitude response as affected by actuators' failures from 1 to 2 orbits: **a** Linear controllers and **b** Nonlinear controllers

ysis of the system indicate that the proposed concept is feasible. Reynold's number on the order of hundreds found by numerical simulation justifies the assumption of laminar flow in the fully filled rings. The fluid rings with natural damping are successful in stabilizing three-dimensional satellite attitude in the Lagrange region. However, the system takes rather long time in the order of tens of orbits to reach steady-state and therefore, it is considered to apply low-powered pumps to regulate the fluid flow inside fluid rings. The proposed linear and nonlinear fluid controllers provide the desired attitude performance in the presence of large attitude disturbances and intermittent actuators' failures. Both the controllers result in the similar attitude performance except for slight variations in fluid torques and flow rates. In the situation of sudden external disturbance torques, the linear fluid controllers are unable to mitigate the disturbance torques resulting in deterioration of attitude performance. On the other hand, the nonlinear controllers are highly successful in maintaining the desired performance with virtually no effect on the satellite attitude response. Thus, the present analysis may serve as a foundation for the implementation of the proposed attitude control method in future satellites.

Acknowledgment The author wishes to acknowledge the financial support for this study provided by Canada Research Chair Program.

References

1. Larson, W.J., Wertz, J.R. (eds.): Space Mission Analysis and Design, 2nd edn. Kluwer, Dordrecht (1992)
2. Wertz, J.R. (ed.): Spacecraft Attitude Determination and Control. D. Reidel, Dordrecht (1978)
3. Sabroff, A.D.: Advanced Spacecraft Stabilization and Control Techniques. AIAA 67–878
4. Kaplan, M.H.: Modern Spacecraft Dynamics and Control. Wiley, New York (1976)
5. Hughes, P.C.: Spacecraft Attitude Dynamics. Wiley, New York (1986)
6. Kumar, K.D., Yasaka, T.: Satellite attitude stabilization through kite-like tether configuration. J Spacecraft Rockets **39**(5), 755–760 (2002)
7. Wolverton, R.W. (ed.): Flight performance handbook for orbital operations: orbital mchanics and astrodynamic formulae, theorems, techniques, and applications. Wiley, New York, pp. 6–32 (1961)
8. Herman, H.H. Jr.: Method and apparatus for movement of liquids by electromagnetic means. US Patent 3,371,541 (1968)
9. Wyatt, T.W., Swet, C.J.: Combined fluid flywheel and propulsion system for spacecraft. US Patent 3,862,732 (1975)
10. Rasmusson, J.K.: Self contained rotator apparatus. US Patent 4,662,178 (1987)
11. Maynard, R.S.: Fluid momentum controller. US Patent 4,776,541 (1988)
12. Lurie, B.J., Schier, J.A., Iskenderian, T.C.: Fluid-loop reaction system. US Patent 5,026,008 (1991)
13. Lurie, B.J., Schier, J.A.: Liquid-ring attitude-control system for spacecraft. NASA Tech. Briefs **14**(9), 82 (1990)
14. Iskenderian, T.C.: Liquid angular-momentum compensator. NASA Tech. Briefs **13**(5), 80 (1989)

15. Laughlin, D.R., Sebesta, H.R., Eckelkamp-Baker, D.: A dual function magnetohydrodynamic (MHD) device for angular motion measurement and control. Adv. Astronaut. Sci. **111**(V), 335–348 (2002)
16. Gilbertson, R.G., Busch, J.D.: A survey of micro-actuator technologies for future spacecraft missions. J. Br. Interplanet. Soc. **49**, 129–138 (1996)
17. Kelly, A., McChesney, C., Smith, P., Walenta, S., Zaruba, C.: A Performance Test of a Fluidic Momentum Controller in Three Axes, Final Report ASE 463Q, Department of Aerospace Engineering Mechanics, The University of Texas, Austin, 7 May 2004
18. Passive Gravity-Gradient Libration Dampers, NASA/SP-8071, NASA space vehicle design criteria (Guidance), NASA (Washington, DC, United States) (1971)
19. Cloop, W., Osborn, L.: Satellite Bus Design for Multiple Satellite System, AIAA/DARPA Meeting on Lightweight Satellite Systems, Monterey, pp. 105–115 (1987)
20. Fleeter, R., Warner, R.: Guidance and control of miniature satellites. In: Nishimura, T. (ed.) Automatic Control in Aerospace: Selected Papers from the IFAC Symposium, Tsukuba, Japan. Pergamon Press, 1990, pp. 243–248 (1989)
21. Martinelli, M.I., Sánchez Peña, R.S.: Passive 3 axis attitude control of MSU-1 pico-satellites. Acta Astronaut **56**, 507–517 (2005)
22. Dally, J.W., Harleman, R.F.: Fluid Dynamics. pp. 259–281. Addison-Wesley, Massachusetts (1966)
23. Perruquetti, W., Barbot, J.P. (eds.) Sliding mode control in engineering. Marcel Dekker, Inc., New York (2002)
24. International Mathematical and Statistical Library (IMSL), Math Library, ver. 3.0. Visual Numerics, Inc., Houston (1997)